ELSEVIER

Journal of Structural Geology 26 (2004) 793–805

JOURNAL OF STRUCTURAL GEOLOGY

www.elsevier.com/locate/jsg

Development of shape- and lattice-preferred orientations of amphibole grains during initial cataclastic deformation and subsequent deformation by dissolution–precipitation creep in amphibolites from the Ryoke metamorphic belt, SW Japan

Reiko Imon[a], Takamoto Okudaira[a,*], Kyuichi Kanagawa[b]

[a]*Department of Geosciences, Osaka City University, Osaka 558-8585, Japan*
[b]*Department of Earth Sciences, Chiba University, Chiba 263-8522, Japan*

Received 5 February 2003; received in revised form 30 July 2003; accepted 4 September 2003

Abstract

Amphibolites from the Ryoke metamorphic belt, SW Japan were deformed initially by cataclasis and subsequently by dissolution–precipitation creep. Initial cataclastic deformation produced a rather weak shape-preferred orientation (SPO) of brown amphibole grains with small aspect ratios as well as a poorly developed amphibole lattice-preferred orientation (LPO) with nα ($\approx a$[100]) axes scattered subnormal to the foliation and nγ or c[001] axes scattered around the lineation. During later deformation by dissolution–precipitation creep, preferential dissolution at grain boundaries subparallel to the foliation and simultaneous compaction normal to the foliation have likely produced a distinct SPO of elongate brown amphibole grains subparallel to the foliation as well as their LPO such that their nγ or c axes are scattered around the lineation, while nα ($\approx a$) and nβ ($= b$[010]) are spread along a girdle normal to the lineation. Also during this deformation green amphibole precipitated as isolated grains or in pressure shadow regions around brown amphibole grains. Nucleation and anisotropic growth of isolated green amphibole grains according to the orientations of the principal stress directions produced an LPO of these grains such that their nα ($\approx a$) are oriented normal to foliation, nβ ($= b$) within the foliation normal to the lineation and nγ (or c) axes are parallel to the lineation. In addition, there is an associated SPO. Growth of green amphibole in pressure shadow regions around brown amphibole grains occurs either syntaxially or anisotropically according to the orientations of the principal stress directions.

Keywords: Amphibole; Cataclasis; Dissolution–precipitation creep; Lattice-preferred orientation; Shape-preferred orientation

1. Introduction

Deformation of the continental crust is thought to be dominated by flow of quartz-rich rocks in the upper crust and flow of feldspar- or hornblende-rich rocks in the lower crust (e.g. Kirby and Kronenberg, 1987; Ranalli and Murphy, 1987). The transition temperature of cataclastic to plastic deformation of quartz is much lower than that of plagioclase or hornblende (Tullis and Yund, 1987, 1992), and plagioclase and hornblende are unlikely to deform plastically in upper crustal conditions. However, such a transition of deformation mechanism with respect to T is applicable only for monomineralic rocks or minerals forming a load-bearing framework (e.g. Handy, 1994). As rocks constituting the upper and lower crusts are polymineralic, their dominant deformation mechanism can be expected to differ from that of monomineralic rocks (e.g. Hacker and Christie, 1990).

Since amphibole may comprise a significant component of the lower crust, its rheological properties are important when considering lower crustal deformation. Lattice-preferred orientations (LPOs) and shape-preferred orientations (SPOs) of amphibole grains hold much information on the kinematics and dynamics of deformed lower crustal rocks. Previous studies of experimentally and naturally deformed amphiboles have suggested that amphibole is one of the strongest minerals, behaving as a rigid inclusion or fracturing during deformation (e.g. Shelley, 1994). Clinoamphibole typically deforms experimentally by twinning on

* Corresponding author.
E-mail address: oku@sci.osaka-cu.ac.jp (T. Okudaira).

0191-8141/$ - see front matter © 2003 Elsevier Ltd. All rights reserved.
doi:10.1016/j.jsg.2003.09.004

($\bar{1}01$) in the $C_{2/m}$ setting up to 600 °C (Rooney et al., 1975; Morrison-Smith, 1976). However, ($\bar{1}01$) twinning has not been reported in naturally deformed clinoamphiboles (Dollinger and Blacic, 1975; Cumbest et al., 1989). Naturally deformed clinoamphiboles exhibit fracturing, bending and kinking on (100)[001] and (100) twinning, whereas plastic strain features such as subgrains and dynamically recrystallized grains are rarely observed (Allison and La Tour, 1977; Biermann and van Roermund, 1983; Cumbest et al., 1989; Nyman et al., 1992). These observations suggest that a dominant deformation mechanism of amphibole grains under crustal conditions is not mainly dominated by plastic intracrystalline process (e.g. Shelley, 1994). On the other hand, Imon et al. (2002) proposed that amphibole as well as plagioclase deformed by dissolution–precipitation creep under upper greenschist–lower amphibolite facies conditions. Wintsch and Yi (2002) also suggested that dissolution–precipitation creep is the important deformation mechanism in wet polyphase rocks under middle crustal conditions.

Deformed amphibolites in a ductile shear zone in the Ryoke metamorphic belt, SW Japan, contain abundant amphibole grains. The deformed amphibolites occur as thin layers (several centimeters thick) within granitic mylonites. In the amphibolites, amphibole grains exhibit a strong shape-preferred orientation parallel to the foliation, which is parallel to the mylonitic foliation of the surrounding granitic mylonites, and to the lithologic contacts. In this study, the shape- and lattice-preferred orientations of amphibole grains are analyzed and discussed in terms of their likely deformation processes.

2. Geological setting and petrography of the amphibolites

2.1. Geological setting

The Cretaceous Ryoke metamorphic belt (Fig. 1a) consists of abundant granitoids and an associated low-*P*/high-*T* metamorphic complex (e.g. Banno and Nakajima, 1992). The EW-trending Ryoke metamorphic belt is juxtaposed against the EW-trending high-*P* Sambagawa metamorphic belt and/or Izumi Group along the Median Tectonic Line (MTL) in SW Japan.

In the northern part of the Kishiwada district (Fig. 1b), foliated granitoids with E–W striking foliation and steep dips are widely distributed. The granitoids are widely mylonitized, and an area of particularly strong mylonitization in the southern part of Kawai is called the Kawai mylonite zone, representing a narrow ENE-trending shear zone (Itihara et al., 1986; Takagi et al., 1988; Fig. 1b). The Kawai mylonite zone and the surrounding highly deformed zone are dominated by granitic mylonites formed under sinistral shear (Takagi et al., 1988). The mylonitic foliation strikes ENE to E and dips 50–70° to the north, and a horizontal stretching lineation trends ENE (Itihara et al., 1986). Along the Tsuda-gawa river section (Fig. 1c), the grain size of minerals constituting the granitic rocks gradually decreases towards the center of the mylonite zone (Takagi et al., 1988; Imon et al., 2002). At the center of the mylonite zone, the granitic ultramylonites exhibit well-developed compositional layering (millimeter scale) defined by alternating quartz-rich and feldspar-rich layers.

2.2. Petrography

Deformed amphibolites occur as thin layers (several centimeters thick) within the granitic mylonites. These amphibolites have been observed throughout the study area from low-strain zones to high-strain zones within and near the Kawai mylonite zone. The deformed amphibolites do not exhibit well-developed compositional layering, yet do show foliation and lineation defined by alignment of plagioclase and amphibole grains, parallel to the foliation and lineation in the surrounding granitic rocks. The amphibolites do not exhibit pinch-and-swell or boudinage structures, even within the high-strain mylonite zone, suggesting that they were internally deformed to the same extent as the surrounding granitic rocks. They may have originally been mafic enclaves, as evidenced by the numerous ellipsoidal inclusions of gabbroic–dioritic composition with granoblastic microstructure in weakly deformed granitic rocks peripheral to the high-strain zone (Itihara et al., 1986).

Amphibolite samples were collected from localities in and near the Kawai mylonite zone along the Tsuda-gawa river section, as shown in Fig. 1c. In this study, four samples (C, H, I and M) were selected for texture analyses. The deformed amphibolite is composed mainly of plagioclase, brown amphibole, green amphibole, chlorite, quartz, titanite with minor K-feldspar, biotite, muscovite, ilmenite, apatite and allanite. Based on the degree of foliation development, the deformed amphibolites can be divided into two types; strongly foliated amphibolites (samples C and M) and weakly foliated amphibolites (samples H and I). The mineral assemblages of the strongly foliated amphibolites do not differ systematically from the weakly foliated ones, although modal abundances of minerals are different between them. Amphibole and plagioclase make up about 60–80 modal percent of all samples. The modal abundances of green amphibole, chlorite and titanite in the strongly

Fig. 1. (a) Index map of Ryoke metamorphic belt, SW Japan. MTL: Median Tectonic Line, ISTL: Itoigawa–Shizuoka Tectonic Line. (b) Geological map of Kishiwada district, Kinki province (modified after Itihara et al., 1986). (c) Route map along Tsuda-gawa river section, showing amphibolite sampling localities.

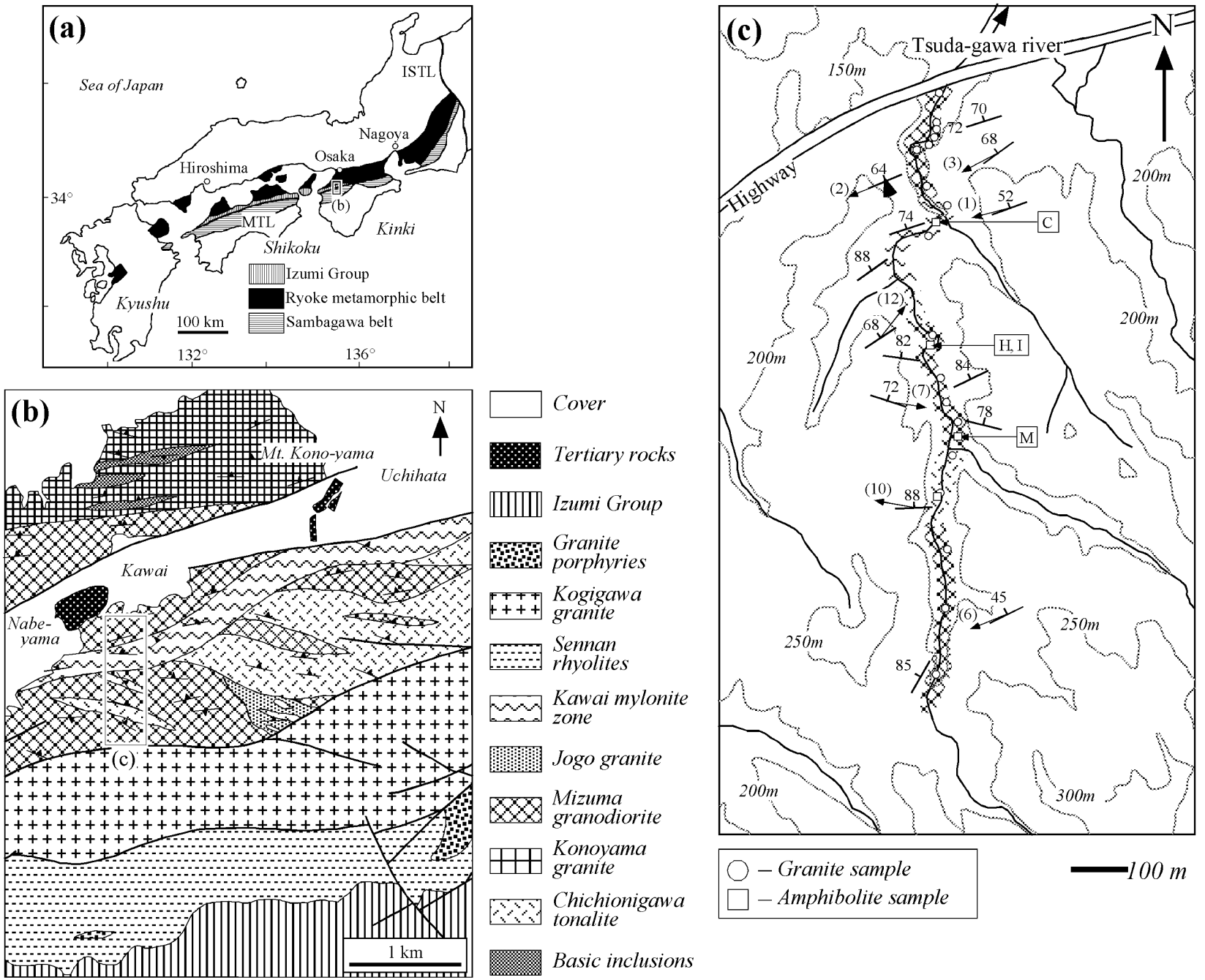
(a)
Sea of Japan
ISTL
Nagoya
Osaka
Hiroshima
34°
(b)
MTL
Kinki
Shikoku
Kyushu
100 km
132°
136°
Izumi Group
Ryoke metamorphic belt
Sambagawa belt
(b)
N
Mt. Kono-yama
Uchihata
Kawai
Nabe-yama
(c)
1 km
Cover
Tertiary rocks
Izumi Group
Granite porphyries
Kogigawa granite
Sennan rhyolites
Kawai mylonite zone
Jogo granite
Mizuma granodiorite
Konoyama granite
Chichionigawa tonalite
Basic inclusions
(c)
Tsuda-gawa river
N
Highway
150m
200m
250m
300m
70
72
68
64
(1)
(2)
(3)
52
74
C
88
(12)
68
82
H, I
84
72
(7)
78
M
(10)
88
45
(6)
85
– Granite sample
– Amphibolite sample
100 m

foliated amphibolites are greater than those in the weakly foliated samples.

Application of the amphibole–plagioclase exchange thermometry of Spear (1980) to the adjacent Ca-poor plagioclase and green amphibole yields temperatures of ca. 510 °C during deformation of the strongly foliated amphibolites (Imon et al., 2002). Although the pressures during deformation cannot be estimated precisely, the lack of metamorphic epidote in the amphibolites suggests that deformation occurred at pressures below 300 MPa (c.f. Spear, 1993).

3. Microstructures and microfabrics

3.1. Microstructures

In the highly deformed zone, strongly foliated amphibolites contain elongated Ti-rich brown amphibole grains rimmed by Ti-poor green amphibole and chlorite (Fig. 2a and b). The foliation is parallel to the mylonitic foliation in the surrounding granite mylonites. C′-type shear bands defined by preferential distribution of the green amphibole, chlorite and titanite occur locally. Amphibole grains rarely show microstructures indicating crystal plasticity such as undulose extinction, deformation lamella, subgrains and grain-boundary migration features (Fig. 2b). Amphibole grains are divided into two types: chemically zoned amphiboles (brown core + green rim) and unzoned green amphiboles. The green rims of zoned amphiboles are preferentially developed in pressure shadow regions around the brown cores, although some green rims are also developed along C′-type shear bands (Fig. 2a). Fig. 3 and Table 1 show the mineral chemistry of amphibole grains in the strongly foliated amphibolite (sample C).

Plagioclase in the strongly foliated amphibolites also consists of two components: a Ca-rich core and a Ca-poor rim. The anorthite-poor plagioclase rims developed in pressure shadow regions around the anorthite-rich cores. Based on these observations, the mass-balance reaction for the deformation event is defined (Imon et al., 2002) as:

$$\text{Ca-rich plagioclase} + \text{Ti-rich brown amphibole} + \text{ilmenite} + \text{quartz} + H_2O \rightarrow \text{Ca-poor plagioclase} + \text{Ti-poor green amphibole} + \text{chlorite} + \text{titanite} \quad (1)$$

As this reaction is a hydration reaction whose products are preferentially distributed in pressure shadow regions, the reaction is considered to have occurred under hydrous, non-hydrostatic conditions.

In the weakly foliated amphibolites, the amphibole and plagioclase grains have angular outlines and straight boundaries (Fig. 2c and d). A few grain-scale faults, as indicated by discrete but small offsets, are observed within some amphibole and plagioclase grains (Fig. 2d).

Table 1
Representative chemical analyses of amphibole (Sample C)

Grain	Zoned		Unzoned
	Brown	Green	Green
wt%			
SiO_2	43.85	46.43	49.32
TiO_2	1.07	0.77	0.20
Al_2O_3	10.30	8.21	4.91
FeO[a]	21.90	20.02	19.57
MnO	0.58	0.69	0.51
MgO	8.83	9.11	10.54
CaO	10.20	10.87	12.24
Na_2O	0.79	0.79	0.50
K_2O	0.49	0.36	0.15
Total	98.01	97.25	97.94
O = 23			
Si	6.60	7.02	7.33
Ti	0.12	0.09	0.02
$^{[4]}Al$	1.40	0.98	0.67
$^{[6]}Al$	0.42	0.48	0.19
Fe^{2+}	2.35	2.51	2.18
Fe^{3+}	0.41	0.02	0.25
Mn	0.07	0.09	0.06
Mg	1.98	2.05	2.34
Ca	1.64	1.76	1.95
Na	0.23	0.23	0.14
K	0.09	0.07	0.03
Mg#[b]	0.46	0.45	0.52

Note: Mineral chemistry was determined using an electron-probe microanalyzer (Shimadzu, EPMA-8705) at Osaka City University. The operating conditions were an accelerating voltage of 15 kV, a beam current of 4 nA and a beam width of 5 μm. X-ray intensities were converted to oxide-weight percentages based on the method of Bence and Albee (1968). Natural and synthetic oxides and silicate minerals were used as standards. Cation contents are assigned using 15 eNK after Leake et al. (1997).

[a] Total Fe as FeO.

[b] Mg#, atomic ratio of $Mg/(Fe^{2+} + Mg)$.

Amphibole grains do not exhibit appreciable chemical zoning, and green amphibole is much less abundant than in the strongly foliated amphibolites.

3.2. Shape-preferred orientation (SPO)

The lengths of the long axis (A) and short axis (B) of each amphibole grain in sections of the selected samples cut perpendicular to the foliation and parallel to the lineation (XZ sections) were measured under an optical microscope, assuming that the grains can be treated as elliptical particles. The grain size (d) of amphiboles is defined as the geometric mean of A and B, that is, $d = \sqrt{(A \times B)}$. Grain size distributions of amphiboles in samples C, H, I and M are shown in Fig. 4. For the strongly foliated samples (C and M), the grain sizes of zoned and unzoned amphiboles have been measured separately (Fig. 4a and b). The average amphibole grain sizes are 107 μm for zoned grains and 41 μm for unzoned green grains in sample C, 161 μm for unzoned brown grains in sample H, 161 μm for unzoned

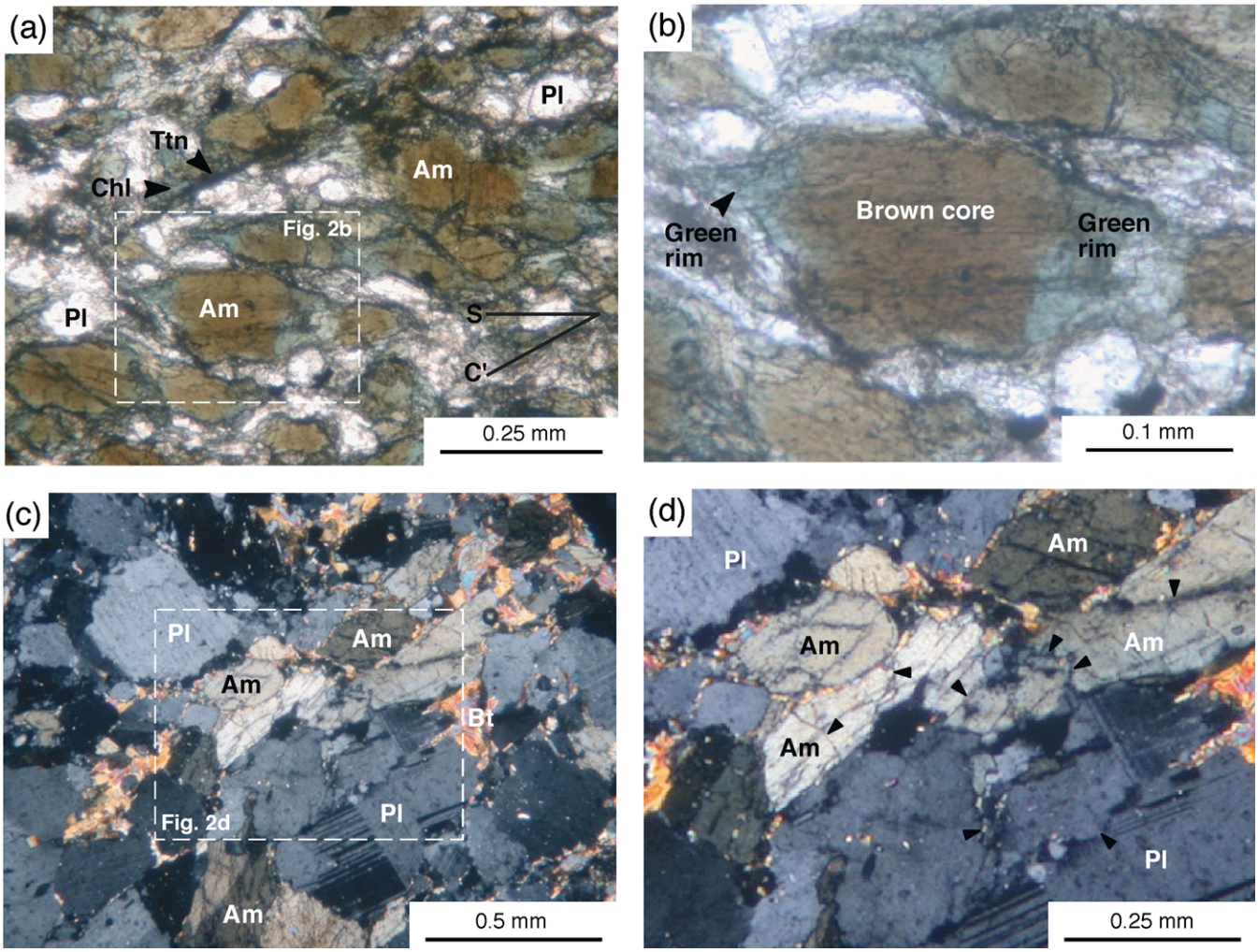

Fig. 2. Photomicrographs showing deformation microstructures of amphibolites (*XZ* sections). (a) and (b) Strongly foliated amphibolite (sample C; plane polarized light). C′-type shear bands indicating sinistral shear are developed, which are composed of green actinolitic ferrohornblende, chlorite and titanite. Amphibole porphyroclasts have brown tschermakitic ferrohornblende cores rimmed by green actinolitic ferrohornblende. The internal asymmetry of sigmoidal shape of the foliation between the C′-planes indicates dextral sense of shear, and the segments between shear bands may have rotated antithetically. (c) and (d) Weakly foliated amphibolite (sample H; cross-polarized light) showing cataclastic features. Plagioclase and amphibole grains are broken and have subangular shapes. Locations of the microcracks and microfaults are indicated by arrows.

brown grains in sample I, and 173 μm for zoned grains and 62 μm for unzoned green grains in sample M. In the strongly foliated samples, the unzoned (green) amphibole grains are finer-grained than the zoned (brown + green) grains which are similar in size to the brown grains in the weakly foliated samples. The brown grains in the weakly foliated amphibolites have a wider range in grain size than the zoned grains in the strongly foliated samples. As in the case of plagioclase grains (Imon et al., 2002), the brown amphibole grains smaller than 100 μm are abundant in the weakly foliated amphibolites, whereas the zoned amphibole grains smaller than 100 μm are less abundant in the strongly foliated amphibolites (see Figs. 2 and 4).

The SPOs of amphibole grains can be shown by their long-axis orientations with respect to the foliation direction (θ), and aspect ratios (R). The long axis orientation of each grain was measured as the angle (anticlockwise positive) from the foliation trace in the *XZ* section to the direction of the long axis (Fig. 5). For the chemically zoned amphibole grains, two sets of data were obtained: the long-axis orientation and aspect ratio of a whole grain (brown core + green rim), and those of its brown amphibole core. Fig. 5 shows the relationships between θ and R in the strongly and weakly foliated amphibolites. In the strongly foliated amphibolites, there is a difference in the $R-\theta$ relation of zoned amphibole grains between samples C and M (Fig. 5a and b). In sample C, the brown amphibole cores have small aspect ratios and show a weak preferred orientation, whereas the whole amphibole grains are preferentially aligned parallel to the foliation. In contrast in sample M, both brown cores and whole grains are preferentially aligned parallel to the foliation. In both samples, grains with aspect ratios smaller than 3 have variable orientations. Among amphibole grains with aspect

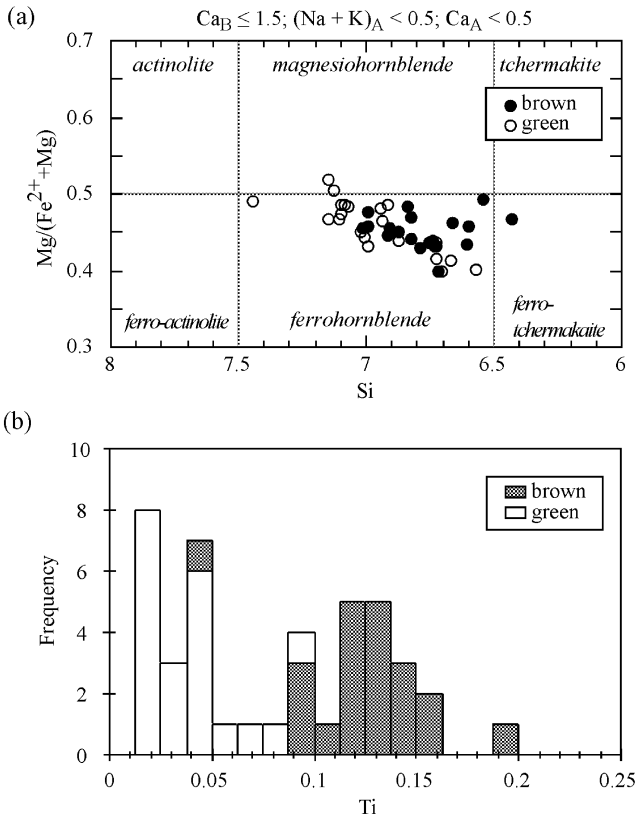

Fig. 3. Chemistry of amphibole grains in the strongly foliated amphibolite (sample C). (a) $Mg/(Fe^{2+} + Mg)$ vs. Si diagram. (b) Frequency diagram of Ti content. Cation proportions are shown for one formula unit. Amphibole classification is according to that of Leake et al. (1997).

ratios larger than 5, unzoned grains are more abundant than zoned grains. Interestingly, the most common long-axis orientation of grains with higher aspect ratios is slightly oblique to the foliation (Fig. 5a and b). This may be due to a modification in SPO caused by the development of C′-shear bands. The maximum aspect ratio in these samples is ≈9 for zoned grains, and ≈14 for unzoned grains.

Although amphibole grains with higher aspect ratios tend to be aligned parallel to the foliation in the weakly foliated amphibolites (samples H and I), the long-axis orientations in these samples are more scattered than in the strongly foliated samples. In addition, the maximum aspect ratios ($R \approx 6$) are smaller, and typically less than 3. Furthermore, grains with low aspect ratios appear randomly oriented.

3.3. Lattice-preferred orientation (LPO)

LPO analyses of amphibole were carried out in *XZ* sections using an optical microscope equipped with a conventional universal stage, and by a scanning electron microscopy (SEM)-based electron backscatter diffraction (EBSD) technique. The optical indicatrix axes of clinoamphibole, nα, nβ and nγ, determined by using a universal stage are related to its crystallographic axes *a*[100], *b*[010] and *c*[001] such that nα is close to *a*, nβ coincides with *b*, and nγ is at an angle of 12°–34° with *c*. Both of the two strongly foliated samples (C and M) exhibit essentially similar amphibole LPOs (Fig. 6a and b). The nγ axes of both zoned and unzoned grains are oriented close to the lineation (*X*). For the unzoned amphiboles, the nα (≈*a*) axes exhibit a weak concentration normal to the foliation (*Z*), and the nβ (= *b*) axes are plotted in the direction perpendicular to the lineation within the foliation (*Y*). The nα and nβ axes for the zoned amphiboles are scattered along a great girdle normal to the *X* direction. The nγ-axis concentration direction and the girdles of nα and nβ are slightly anticlockwise oblique to the *X* direction and the *X*-normal girdle, respectively (Fig. 6a and b), which may be due to a modification in LPO caused by the development of C′-shear bands which also affected SPO.

Fig. 6 also shows the relationship between the optical indicatrix axis orientations and aspect ratios in the strongly foliated samples C and M. The nγ axes of the more elongated brown cores tend to be more concentrated in the *X* direction than those of the less elongated cores, while the nα and nβ axes of the more elongated brown cores have a tendency to be more concentrated in the *Z* and *Y* directions, respectively, than those of the less elongated cores. In contrast, in the green amphibole rims and unzoned grains, no clear correlation is found between the optical indicatrix axis orientations and the aspect ratios (Fig. 6a and b).

In the weakly foliated amphibolites (samples H and I), the amphibole optical indicatrix axes exhibit rather weak preferred orientations such that nα axes are scattered around the *Z* directions (Fig. 6c and d). In addition, nβ and nγ axes tend to be scattered around the *Y* and *X* directions, respectively, in sample H, while they tend to be variably oriented subparallel to the *XY* plane in sample I.

Amphibole LPO data of sample C were also obtained by the EBSD technique. This technique allows the complete crystallographic orientation of grains on the surface of a polished sample to be determined with spatial resolution of about 1 μm and an absolute angular resolution of 1° (Prior et al., 1996). This technique has become widely used for textural analysis of deformed rocks (Prior et al., 1999). The *XZ* section of sample C was polished using diamond paste on a paper lap followed by chemical polishing using a colloidal silica suspension in order to remove any surface damage, and then coated with a thin carbon layer (about 5 nm) to reduce specimen charging. EBSD patterns were collected using a JEOL JSM-5600 scanning electron microscope at Chiba University with an accelerating voltage of 17 kV and a beam current of approximately 3.5–3.8 nA. The sample was tilted to 73° in the microscope chamber. The EBSD patterns were indexed using Channel 5 Software of HKL Technology. Amphibole cores and rims were measured separately. The results are similar to those obtained by universal stage measurements (see Figs. 6a and 7). The crystallographic *c*[001] axes of brown cores and green rims in sample C are oriented in the *X* direction

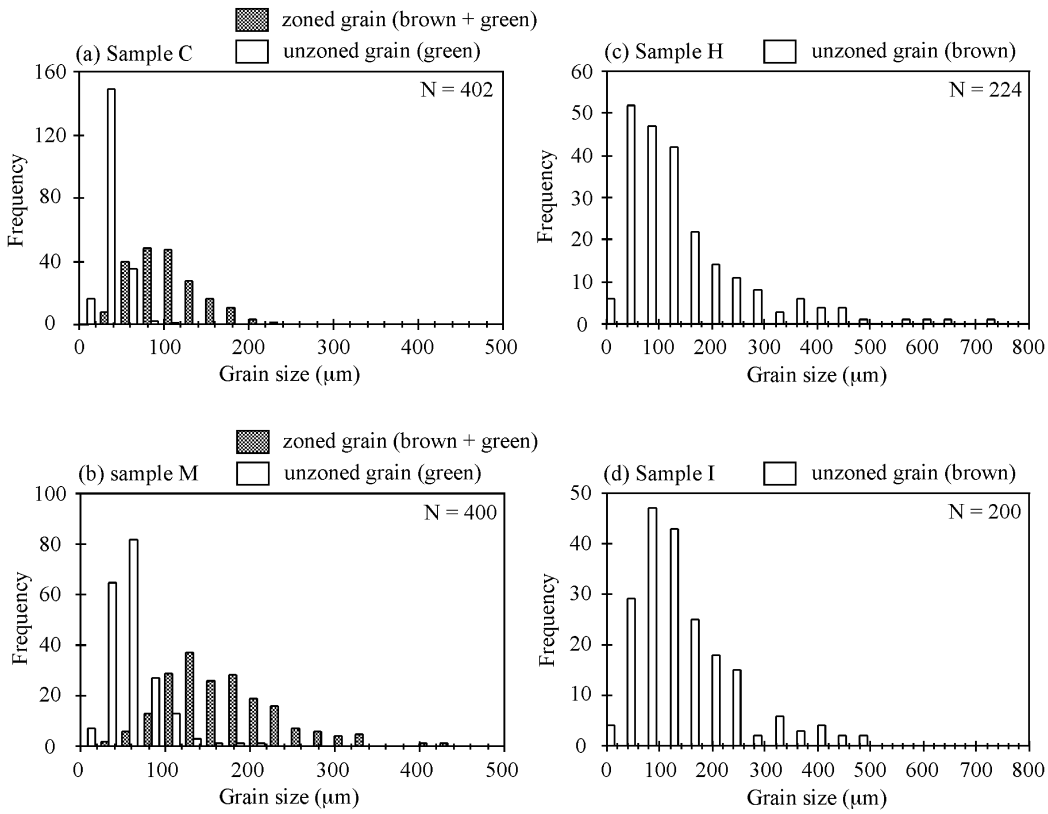

Fig. 4. Frequency diagram showing amphibole grain size distributions in two strongly foliated samples (C and M) and two weakly foliated samples (H and I).

(Fig. 7). The *a*[100] axes are spread along a great girdle around the *X* direction, with a weak tendency to be scattered around the *Z* direction. The *b*[010] axes are oriented quite variably, but have a weak tendency to be scattered around the *Y* direction. Although there is a correlation between crystallographic orientations and the aspect ratios in the results obtained by universal stage measurements, the correlation is not so clear in the results of EBSD analysis. This may be due to the smaller number of EBSD data, especially for grains with higher aspect ratios.

The relationship in each zoned grain of sample C between the brown core *c* axis with respect to the lineation *X* and the internal angle between the *c* axes of the brown core and green rim is shown in Fig. 8. There are zoned grains plotted near abscissa in Fig. 8 with approximately the same core and rim *c*-axis orientations irrespective of their core *c*-axis orientations, while in other zoned grains the internal angle between the core and rim *c* axes tends to increase with the core *c*-axis orientation going away from *X*.

4. Discussion

4.1. Deformation processes in the deformed amphibolites

In the weakly foliated amphibolites, brown amphibole and plagioclase grains have angular outlines and straight boundaries (Fig. 2c and d). Many microcracks and microfaults can also be recognized. In addition, the amphibole grain-size distributions with a small number of large grains and a large number of small grains (Fig. 4c and d) are consistent with grain-size reduction due to microcracking and comminution (e.g. Passchier and Trouw, 1996, p. 25). All of these are suggestive of cataclastic deformation, since the deformed amphibolites may have originally been mafic enclaves having granoblastic microstructure. The weakly foliated amphibolites are therefore likely deformed predominantly by cataclasis.

In the strongly foliated amphibolites, amphibole grains do not show such cataclastic microstructures as observed in the weakly foliated amphibolites (Fig. 2a and b). They also rarely show such microstructures as undulose extinction, deformation lamella, subgrains and grain-boundary migration features (Fig. 2b), and hence they are unlikely to have been deformed by crystal plasticity. In fact, it is generally accepted that amphibole is the least plastic among common rock-forming silicate minerals under crustal conditions (e.g. Shelley, 1994). The deformation temperatures of ca. 510 °C (Imon et al., 2002) estimated for the studied amphibolites may be too low for amphibole to deform by crystal plasticity.

Green amphibole in the strongly foliated amphibolites is a product of the reaction (1), and occurs as either unzoned grains or in pressure shadow regions around brown amphibole grains. The latter occurrence suggests precipitation of green amphibole in low normal-stress regions, in the same

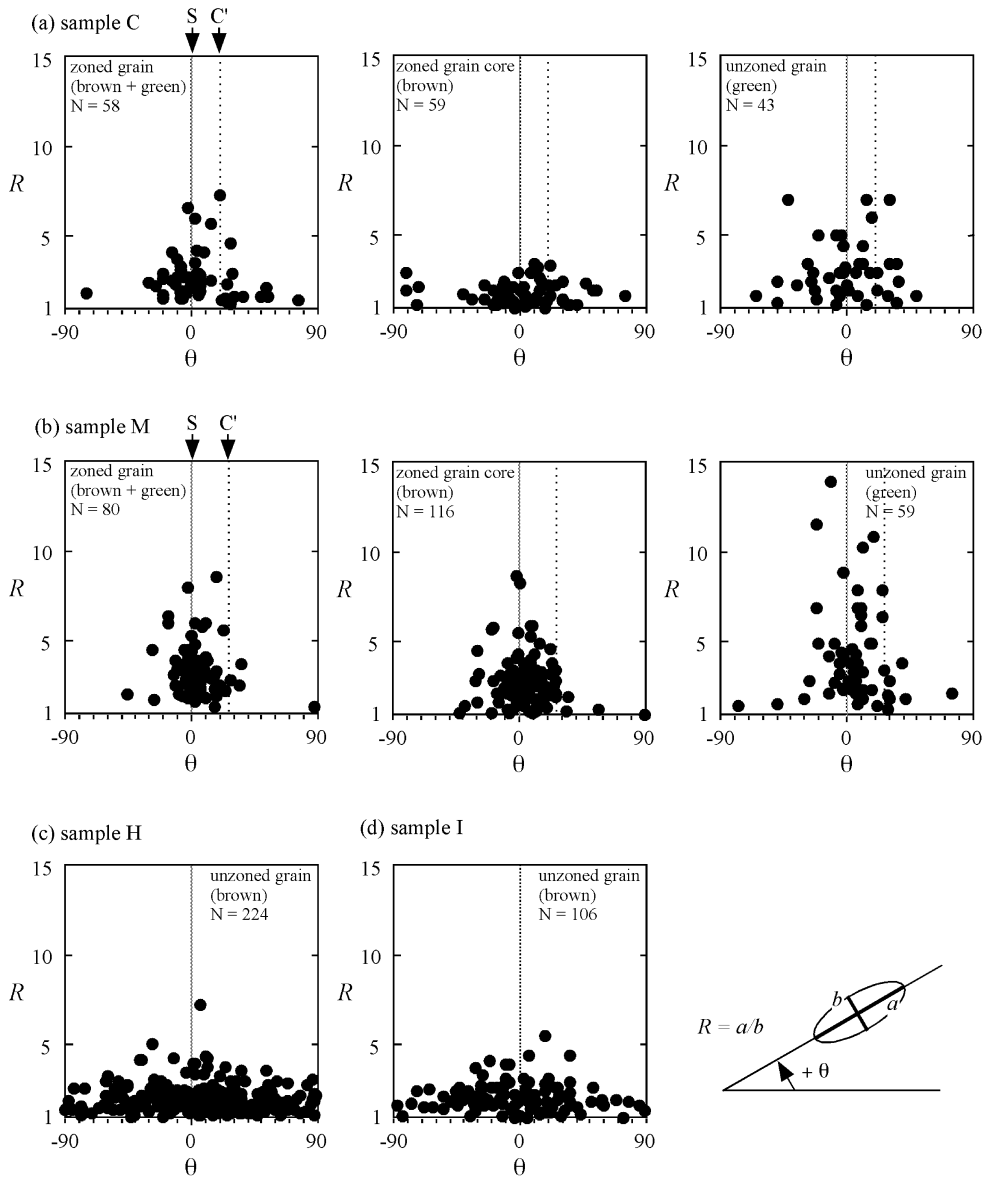

Fig. 5. Amphibole aspect ratios (R) and long-axis orientations (θ) in the XZ section. (a) and (b) Strongly foliated amphibolites (samples C and M). (c) and (d) Weakly foliated amphibolites (samples H and I). θ is measured anticlockwise positive from the foliation trace (S). C′ denotes the orientation of C′-type shear bands.

way as that of Ca-poor plagioclase precipitation around Ca-rich plagioclase grains in the same amphibolites (Imon et al., 2002). The reaction (1) may therefore be an incongruent pressure solution by which Ti-rich brown amphibole and Ca-rich plagioclase grains dissolve at their high-normal stress grain boundaries parallel to the foliation, and Ti-poor green amphibole and Ca-poor plagioclase precipitate in pressure shadow regions around brown amphibole and Ca-rich plagioclase grains, respectively. Thus dissolution–precipitation creep probably plays an important role in ductile deformation of the strongly foliated amphibolites.

Because characteristic microstructures of the deformed amphibolites change from cataclastic to ductile with increasing strain (Fig. 2), it is likely that initial cataclastic deformation has been followed by dissolution–precipitation creep in the strongly foliated amphibolites (Imon et al., 2002), and that the brown amphibole cores in the strongly foliated amphibolites have originated from cataclastically deformed amphibole grains such as those in the weakly

Fig. 6. Lower-hemisphere, equal-area projections showing the orientations of amphibole optical indicatrix axes of nα, nβ and nγ. (a) and (b) Strongly foliated amphibolites. (c) and (d) Weakly foliated amphibolites. Grains with low ($R \leq 3$) and high ($R > 3$) aspect ratios are indicated by closed and open circles, respectively. S and C′ denote the orientation of the foliation and C′-type shear bands, respectively.

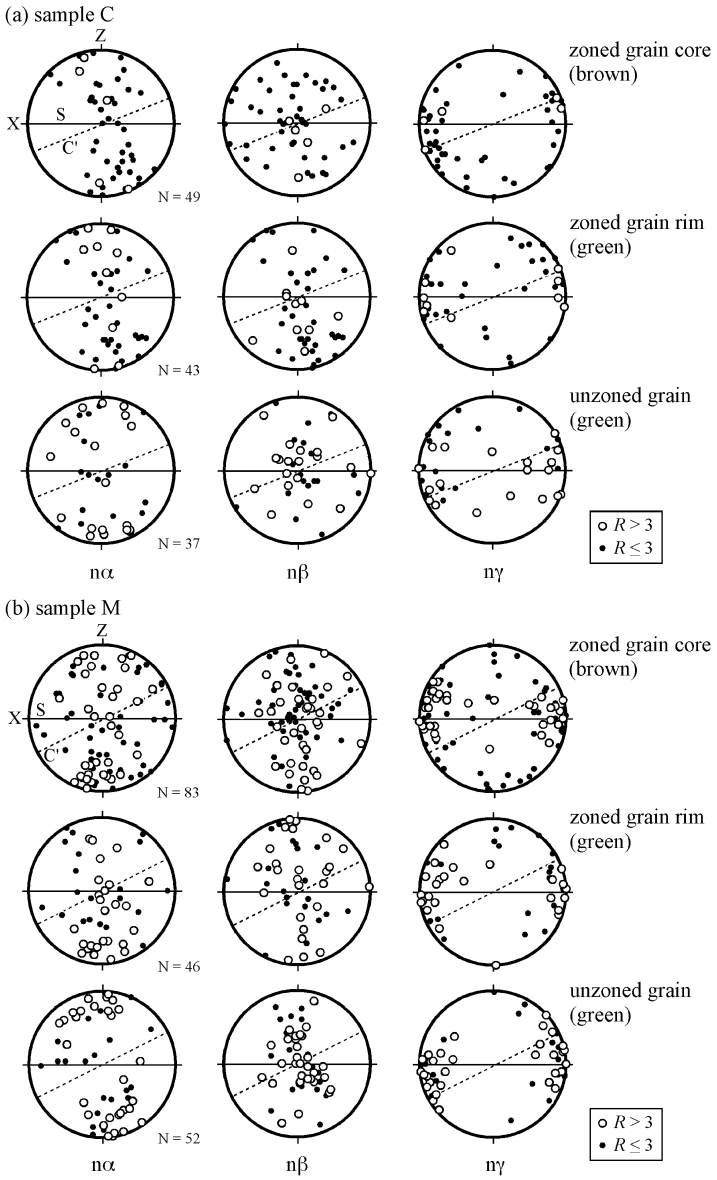
(a) sample C
Z
X
S
C'
N = 49
N = 43
N = 37
zoned grain core (brown)
zoned grain rim (green)
unzoned grain (green)
R > 3
R ≤ 3
nα
nβ
nγ
(b) sample M
Z
X
S
C'
N = 83
N = 46
N = 52
zoned grain core (brown)
zoned grain rim (green)
unzoned grain (green)
R > 3
R ≤ 3
nα
nβ
nγ
(c) sample H (unzoned brown amphiboles)
Z
X
S
N = 124
nα
nβ
nγ
(d) sample I (unzoned brown amphiboles)
Z
X
S
N = 192
nα
nβ
nγ

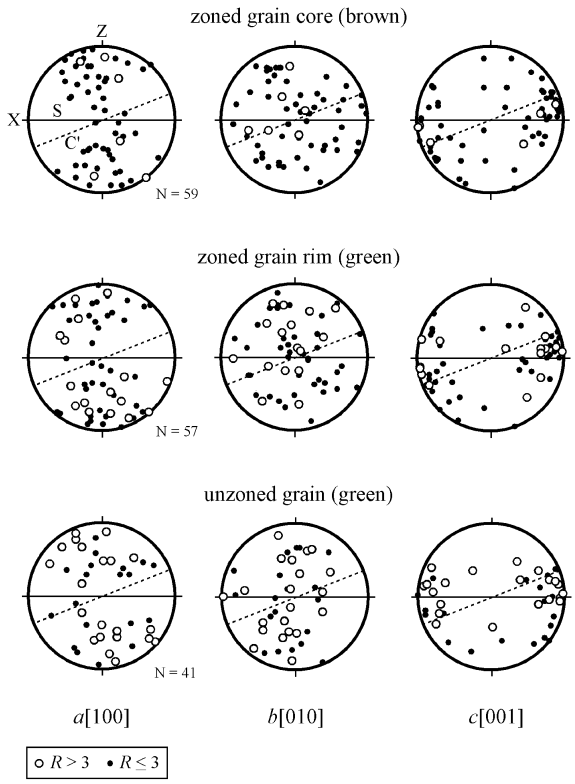

Fig. 7. Lower-hemisphere, equal-area projections showing the orientations of amphibole crystallographic axes of a[100], b[010] and c[001] in sample C. Grains with low ($R \leq 3$) and high ($R > 3$) aspect ratios are indicated by closed and open circles, respectively. S and C′ denote the orientation of the foliation and C′-type shear bands, respectively.

deformed amphibolites. Available data suggest that the strongly foliated amphibolites contain less abundant fine brown-amphibole grains than those in the weakly foliated amphibolites (cf. Figs. 2 and 4), and this is probably because fine brown-amphibole grains in the former have been reduced in number by dissolution. The initial cataclastic deformation such as fracturing and comminution of amphibole and plagioclase grains would draw fluid into the cataclastic zone (e.g. Matthäi and Roberts, 1997), which is required for the hydration reaction (1). Such deformation-induced fluid flux is also important in metamorphic re-equilibration and mass transport required for dissolution–precipitation of amphibole and plagioclase grains.

Thus fluid infiltration during the initial cataclastic deformation may have promoted subsequent deformation by dissolution–precipitation creep of the studied amphibolites at pressures below 300 MPa and temperatures of ca. 500 °C. The microstructural change from cataclastic to ductile in these amphibolites probably represents a transition in dominant deformation mechanism from cataclasis to dissolution–precipitation creep. Although brittle–ductile transition from cataclasis to dislocation creep is generally accepted (e.g. Kohlstedt et al., 1995), our study therefore suggests another brittle–ductile transition from cataclasis to dissolution–precipitation creep occurring in the middle crust. In the latter case, the crustal strength would be

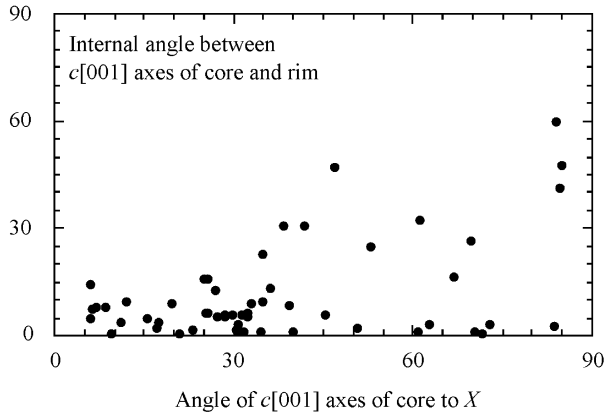

Fig. 8. Relationship in sample C between the orientation of brown core c[001] axis with respect to mineral lineation X and the internal angle between c[001] axes of brown core and green rim.

significantly different from that in the former case (Wintsch and Yi, 2002).

4.2. Development of shape- and lattice-preferred orientations of amphibole grains

In the weakly foliated amphibolites predominantly deformed by cataclasis, cataclastic deformation has probably produced a rather weak SPO and a poorly developed LPO of brown amphibole grains (Figs. 5c and d and 6c and d). As shown in Fig. 6c and d, the observed LPO pattern is such that nα ($\approx a$[100]) axes are oriented subnormal to the foliation ($\approx Z$). The nβ ($= b$[010]) axes are scattered around the lineation-normal direction within the foliation (Y). The nγ axes exhibit a weak concentration around the lineation (X) (Fig. 6c) or subparallel to the foliation ($\approx XY$) (Fig. 6d). Allison and La Tour (1977) have reported an LPO of cataclastically deformed hornblende grains with their c[001] axes away from the foliation due to rotation of fragments bounded by planes subnormal to the c axis. But this is not the case for amphibole grains in the weakly foliated amphibolites studied, where their nγ axes and hence c axes are oriented subparallel to the foliation. The reason for the development of the observed LPO pattern during cataclastic deformation of brown amphibole grains in the weakly foliated amphibolites is unknown at present.

The unzoned green amphibole grains in the strongly foliated amphibolites have nucleated and grown by the reaction (1), and their SPO and LPO can be produced by anisotropic growth during deformation by dissolution–precipitation creep (c.f. Shelley, 1994; Bons and den Brok, 2000; Heidelbach et al., 2000). Schwerdtner (1964) and Hara et al. (1983) have advocated a mechanism whereby amphibole c axis preferentially grows in the direction of the minimum principal stress. The unzoned green amphibole grains exhibit an LPO such that their nα ($\approx a$), nβ ($= b$) and nγ (or c) axes are oriented in the Z, Y and X directions, respectively (Figs. 6a and b and 7).

The X direction should be subparallel to the minimum principal stress direction in the strongly foliated amphibolites, because this is the direction where green amphibole precipitated around brown amphibole grains. This relationship is suggested by the other microstructural features. As shown in Fig. 2a, the internal asymmetry of sigmoidal shape of the foliation between the C′-planes indicates dextral sense of shear, while the external asymmetry of angle between the enveloping surface of the foliation and the shear bands indicates sinistral sense of shear. The segments between shear bands may have rotated antithetically in the stretching shear zones, whereas the bands must have rotated synthetically if flow in a shear zone is a simple shear (Passchier and Trouw, 1996, p. 113). The C′-planes in the strongly foliated amphibolites, therefore, are extensional crenulation cleavage of Platt and Vissers (1980). In such stretching shear zones, two sets of conjugate shear bands would be expected around the shortening instantaneous stretching axis (ISA), but only one, at a small angle to the foliation is realized (Passchier, 1991). The shortening ISA located at high angle to the foliation and the extensional ISA oriented subparallel to the foliation (= lateral extension of the shear zone). Therefore, in the strongly foliated amphibolites, the stretching ISA is roughly parallel to the lineation, and may be parallel to the minimum principal stress direction. The observed LPO of unzoned green amphibole grains is therefore consistent with anisotropic amphibole growth according to the orientations of the principal stress directions. The SPO of unzoned green amphibole grains such that their long axes parallel to their c axes are preferentially oriented parallel to the X direction (Fig. 5a and b) is a necessary consequence of such anisotropic growth. It should be noted that our data suggest that amphibole a and b axes preferentially grow in the maximum and intermediate principal stress directions, respectively.

In principle, anisotropic growth should also apply to the green amphibole rims of zoned grains, because they also have grown by the reaction (1). The LPO of green amphibole rims is such that the c or nγ axis is oriented in the X direction and the a ($\sim$nα) and b (= nβ) axes are oriented along a girdle around the X direction, which is basically the same as that of brown amphibole cores (Figs. 6a and b and 7). Unlike the green amphibole rims, the LPO patterns of unzoned green amphiboles resemble point-maximum patterns. This implies that the growth of green amphibole rims is primarily controlled by crystallographic orientations of brown amphibole cores rather than by the principal stress directions, i.e. syntaxial. Green amphibole rims with approximately the same crystallographic orientations as brown amphibole cores irrespective of their orientations, such as those plotted near abscissa in Fig. 8, represent syntaxially grown rims. Fig. 8 also shows the presence of green rims with their c axes away from those of brown cores oblique to the X direction. This implies that the c axes of these green rims keep close to the X direction irrespective of their brown core orientations. These green amphibole rims have likely grown anisotropically with their c axes parallel to the X direction as unzoned green amphibole grains. The distinct SPO of zoned grains in sample C may be due to this anisotropic growth of green rims, because that of brown cores in this sample is rather weak (Fig. 5a).

The brown amphibole cores in the strongly foliated amphibolites probably have been inherited from cataclastically deformed amphibole grains such as those in the weakly deformed amphibolites, as discussed above. The brown amphibole cores in sample C have relatively small aspect ratios and exhibit a weak SPO similar to those of brown amphibole grains in the weakly foliated amphibolites (Fig. 5a, c and d). Although the brown amphibole cores in sample M exhibit a distinct SPO, those with small aspect ratios are variably oriented (Fig. 5b). In addition, the brown amphibole cores with small aspect ratios ($R \leq 3$) in both samples C and M exhibit an LPO such that a ($\sim$nα), b (= nβ) and c or nγ axes are weakly oriented in the Z, Y and X directions, respectively (Figs. 6a and b and 7), which is also similar to that of the weakly foliated sample H (Fig. 6c). Hence the brown amphibole cores with small aspect ratios in the strongly foliated amphibolites may preserve the SPO and LPO produced during initial cataclastic deformation, which have not been largely modified by later deformation by dissolution–precipitation creep.

In contrast, the brown amphibole cores with large aspect ratios ($R > 3$) in the strongly foliated amphibolites exhibit a distinct SPO and an LPO such that a ($\sim$nα) and b (= nβ) axes are spread along a girdle around the X direction (Figs. 6a and b and 7), both of which are different from those of the weakly foliated amphibolites. Such SPO and LPO of elongate brown amphibole cores may have been produced during initial cataclastic deformation by rigid-body rotation in cataclastically flowing fine-grained matrix produced by fracturing and comminution. The rigid-body rotation of elongate brown amphibole clasts subparallel to their c axes would have resulted in their preferential alignment subparallel to the lineation X around which their a and b axes are variably oriented. A similar mechanism for preferential alignment of elongate clasts in cataclastically flowing fine-grained matrix has also been reported from experimentally and naturally deformed rocks (e.g. Tullis and Yund, 1987, 1992; Tanaka, 1992). The difference in brown core SPO between samples C and M (Fig. 5a and b) may then be due to the difference in cataclastic strain, i.e. cataclastic strain of sample M being larger than that of sample C. However, this is inconsistent with the observation that zoned grains in sample M are significantly coarser-grained than those in sample C (Fig. 4), because a higher cataclastic strain should result in a finer grain-size distribution. The SPO and LPO development of elongate brown amphibole cores during initial cataclastic deformation is therefore problematic.

Alternatively, the SPO and LPO of the elongate brown amphibole cores may have been produced during later

deformation by dissolution–precipitation creep. Preferential dissolution of brown amphibole clasts along high normal-stress boundaries, i.e. along grain boundaries subparallel to the foliation, possibly produced elongate brown amphibole grains with their SPO subparallel to the foliation, which may have been further enhanced by compaction associated with dissolution–precipitation creep. Although preferential dissolution alone does not necessarily produce an LPO, the pre-existing weak LPO with *c* or nγ axis scattered around the *X* direction as those in the weakly foliated amphibolites could have been modified to more distinct point-maximum pattern, and *a* and *b* axes could have been rotated around the *c* axis during the associated compaction. The difference in brown core SPO between samples C and M (Fig. 5a and b) may then be due to their difference in strain during deformation by dissolution–precipitation creep. In fact, the smaller aspect ratios and weaker SPO of unzoned green amphibole grains in sample C than those in sample M (Fig. 5a and b) indicate that the strain during deformation by dissolution–precipitation creep is smaller in sample C than in sample M.

Acknowledgements

N. Aikawa and K. Ishii are appreciated for comments and encouragement. The paper benefited substantially from detailed reviews by T.E. La Tour and D. Shelley. J. Hippertt is thanked for the editorial handling of the paper. This study was financially supported by the Grants-in-Aid for Scientific Research (14740305) from the Japan Society for the Promotion of Science to T. Okudaira.

References

Allison, I., La Tour, T.E., 1977. Brittle deformation of hornblende in a mylonite: a direct geometrical analogue of ductile deformation by transition gliding. Canadian Journal of Earth Sciences 14, 1953–1958.

Banno, S., Nakajima, T., 1992. Metamorphic belts of Japanese Islands. Annual Reviews of Earth and Planetary Sciences 20, 159–179.

Bence, A.E., Albee, A.L., 1968. Empirical correction factors for the electron microanalysis of silicates and oxides. Journal of Geology 76, 382–403.

Biermann, C., van Roermund, H.L.M., 1983. Defect structures in naturally deformed clinoamphiboles—a TEM study. Tectonophysics 95, 267–278.

Bons, P.D., den Brok, B., 2000. Crystallographic preferred orientation development by dissolution–precipitation creep. Journal of Structural Geology 22, 1713–1722.

Cumbest, R., Drury, M.R., van Roermund, H.L., Simpson, C., 1989. Dynamic recrystallization and chemical evolution of clinoamphibole from Senja, Norway. Contributions to Mineralogy and Petrology 101, 339–349.

Dollinger, G., Blacic, D.L., 1975. Deformation mechanisms in experimentally and naturally deformed amphibolites. Earth and Planetary Science Letters 26, 409–416.

Hacker, B.R., Christie, J.M., 1990. Brittle/ductile and plastic/cataclastic transition in experimentally deformed and metamorphosed amphibolite. In: Duba, A.G., Durham, W.B., Handin, J.W., Wang, H.F. (Eds.), The Brittle–Ductile Transition in Rocks. AGU Geophysical Monograph 56, pp. 127–148.

Handy, M.R., 1994. Flow laws for rocks containing two non-linear viscous phases: a phenomenological approach. Journal of Structural Geology 16, 287–301.

Hara, I., Shiota, T., Maeda, M., Miyaoka, H., 1983. Deformation and recrystallization of amphiboles in Sambagawa schist, with special reference to history of Sambagawa metamorphism. Journal of Science, Hiroshima University, Series C 8, 135–148.

Heidelbach, F., Post, A., Tullis, J., 2000. Crystallographic preferred orientation in albite samples deformed experimentally by dislocation and solution precipitation creep. Journal of Structural Geology 22, 1649–1661.

Imon, R., Okudaira, T., Fujimoto, A., 2002. Dissolution and precipitation processes in the deformed amphibolites: an example from the ductile shear zone of the Ryoke metamorphic belt, SW Japan. Journal of Metamorphic Geology 20, 297–308.

Itihara, M., Ichikawa, K., Yamada, N., 1986. Geology of the Kishiwada district. Quadrangle series, scale 1:50,000, Geological Survey of Japan, Tsukuba (in Japanese with English abstract).

Kirby, S.H., Kronenberg, A.K., 1987. Rheology of the lithosphere: selected topics. Reviews in Geophysics 25, 3177–3192.

Kohlstedt, D.L., Evans, B., Mackwell, S.J., 1995. Strength of the lithosphere: constraints imposed by laboratory experiments. Journal of Geophysical Research 100, 17587–17602.

Leake, B.E., Woolley, A.R., Arps, C.E.S., et al., 1997. Nomenclature of amphiboles. Report of the Subcommittee on Amphiboles of the International Mineralogical Association, Commission on New Minerals and Mineral Names. American Mineralogist 82, 1019–1037.

Matthäi, S.K., Roberts, S.G., 1997. Transient versus continuous fluid flow in seismically active faults: an investigation by electric analogue and numerical modelling. In: Jamtveit, B., Yardley, B. (Eds.), Fluid Flow and Transport in Rocks: Mechanisms and Effects, Chapman & Hall, London, pp. 263–295.

Morrison-Smith, D.J., 1976. Transmission electron microscopy of experimentally deformed hornblende. American Mineralogists 61, 272–280.

Nyman, M.W., Law, R.D., Smelik, E.A., 1992. Cataclastic deformation mechanism for the development of core–mantle structure in amphibole. Geology 20, 455–458.

Passchier, C.W., 1991. Geometric constraints on the development of shear bands in rocks. Geologie En Mijnbouw 70, 203–211.

Passchier, C.W., Trouw, R.A.J., 1996. Microtectonics, Springer-Verlag, Berlin, Heidelberg, 289pp.

Platt, J.P., Vissers, R.L.M., 1980. Extensional structures in anisotropic rocks. Journal of Structural Geology 2, 397–410.

Prior, D.J., Trimby, P.W., Weber, U.D., Dingley, D., 1996. Orientation contrast imaging of microstructures in rocks using forescatter detectors in the scanning electron microscope. Mineralogical Magazine 60, 859–869.

Prior, D.J., Boyle, A.P., Brenker, F., et al., 1999. The application of electron backscatter diffraction and orientation contrast imaging in the SEM to textural problems in rocks. American Mineralogist 84, 1741–1759.

Ranalli, G., Murphy, D.C., 1987. Rheological stratification of the lithosphere. Tectonophysics 132, 281–295.

Rooney, T.P., Riecker, R.E., Gavasci, A.T., 1975. Hornblende deformation features. Geology 3, 364–366.

Schwerdtner, W.M., 1964. Preferred orientation of hornblende in a banded hornblende gneiss. American Journal of Science 262, 1212–1229.

Shelley, D., 1994. Spider texture and amphibole preferred orientations. Journal of Structural Geology 16, 709–717.

Spear, F.S., 1980. NaSi ↔ CaAl exchange equilibrium between plagioclase and amphibole. Contributions to Mineralogy and Petrology 72, 33–41.

Spear, F.S., 1993. Metamorphic Phase Equilibria and Pressure–Temperature–Time Path, Mineralogical Society of America, Washington DC, 799pp.

Takagi, H., Mizutani, T., Hirooka, K., 1988. Deformation of quartz in an

inner shear zone of the Ryoke belt—an example in the Kishiwada area, Osaka Prefecture. Journal of the Geological Society of Japan 94, 869–886 (in Japanese with English abstract).

Tanaka, H., 1992. Cataclastic lineation. Journal of Structural Geology 14, 1239–1252.

Tullis, J., Yund, R.A., 1987. Transition from cataclastic flow to dislocation creep of feldspar: mechanisms and microstructures. Geology 15, 606–609.

Tullis, J., Yund, R.A., 1992. The brittle–ductile transition in feldspar aggregate: an experimental study. In: Evans, B., Wong, T.F. (Eds.), Fault Mechanics and Transport Properties of Rocks: A Festschrift in Honor of W.F. Brace, Academic Press, London, pp. 90–117.

Wintsch, R.P., Yi, K., 2002. Dissolution and replacement creep: a significant deformation mechanism in mid-crustal rocks. Journal of Structural Geology 24, 1179–1193.